Published in final edited form as:

Nature. 2012 July 12; 487(7406): 239–243. doi:10.1038/nature11125.

The Mutational Landscape of Lethal Castrate Resistant Prostate Cancer

Catherine S. Grasso[1,2,#], **Yi-Mi Wu**[1,2,#], **Dan R. Robinson**[1,2,#], **Xuhong Cao**[1,6], **Saravana M. Dhanasekaran**[1,2], **Amjad P. Khan**[1,2], **Michael J. Quist**[1,2], **Xiaojun Jing**[1,2], **Robert J. Lonigro**[1,5], **J. Chad Brenner**[1], **Irfan A. Asangani**[1,2], **Bushra Ateeq**[1,2], **Sang Y. Chun**[1], **Javed Siddiqui**[1,2], **Lee Sam**[1], **Matt Anstett**[9], **Rohit Mehra**[1,2], **John R. Prensner**[1,2], **Nallasivam Palanisamy**[1,2,5], **Gregory A. Ryslik**[7], **Fabio Vandin**[8], **Benjamin J. Raphael**[8], **Lakshmi P. Kunju**[1,2], **Daniel R. Rhodes**[1,2,9], **Kenneth J. Pienta**[1,3,4,5,*], **Arul M. Chinnaiyan**[1,2,4,5,6,*], and **Scott A. Tomlins**[1,2]

[1]Michigan Center for Translational Pathology, University of Michigan Medical School, Ann Arbor, MI, USA

[2]Department of Pathology, University of Michigan Medical School, Ann Arbor, MI, USA

[3]Department of Internal Medicine, University of Michigan Medical School, Ann Arbor, MI, USA

[4]Department of Urology, University of Michigan Medical School, Ann Arbor, MI, USA

[5]Comprehensive Cancer Center, University of Michigan Medical School, Ann Arbor, MI, USA

[6]Howard Hughes Medical Institute, University of Michigan Medical School, Ann Arbor, MI, USA

[7]Division of Biostatistics, Yale School of Public Health, New Haven, CT, USA

[8]Department of Computer Science & Center for Computational Molecular Biology, Brown University, Providence, RI, USA

[*]Corresponding authors: Kenneth J. Pienta, M.D., American Cancer Society Professor, Professor of Internal Medicine and Urology, Comprehensive Cancer Center, kpienta@med.umich.edu. Arul M. Chinnaiyan, M.D., Ph.D., Investigator, Howard Hughes Medical Institute, American Cancer Society Professor, S. P. Hicks Endowed Professor of Pathology, Professor of Pathology and Urology, Comprehensive Cancer Center, arul@umich.edu, University of Michigan Medical School, 1400 E. Medical Center Dr. 5316 CCGC, Ann Arbor, MI 48109-0602.

[#]These authors contributed equally

Conflict of interest

The University of Michigan has been issued a patent on the detection of ETS gene fusions in prostate cancer, on which S.A.T., R.M., D.R.R. and A.M.C. are listed as co-inventors. The University of Michigan licensed the diagnostic field of use to Gen-Probe, Inc. S.A.T. has served as a consultant to Compendia Biosciences and has received honoraria from Ventana/Roche. A.M.C. has served as a consultant for Gen-Probe, Inc. and Ventana/Roche. D.R.R. and A.M.C. are co-founders of Compendia Biosciences, which licensed Oncomine from the University of Michigan. M.A. is an employee of Compendia Biosciences. The remaining authors declare no conflicts of interest.

Statement of Work

S.A.T., K.J.P., and A.M.C. conceived the study. K.J.P. established the rapid autopsy program and K.J.P., R.M., J.S., L.P.K. and S.A.T. carried out rapid autopsies and assisted in tissue procurement and analysis. Y.W., D.R., X.C., N.P., and X.J. isolated DNA and RNA and carried out whole exome and transcriptome sequencing. X.J. and X.C. performed gene expression and aCGH. C.G., M.Q., L.S., R.J.L., G.A.R., F.V., B.J.R., and S.A.T. carried out bioinformatics and biostatistical analysis of sequencing data. Y.W., S.M.D., D.R., and S.Y.C. carried out Sanger sequencing based validation. R.J.L., M.A., D.R.R., X.C., X.J., and S.A.T. analyzed gene expression profiling and aCGH data. A.P.K. and J.R.P. carried out studies on AR interactions and function. I.A.A. carried out *ETS2* studies and Y.W., B.A., D.R., and J.C.B. carried out *FOXA1* studies. S.A.T., C.S.G. and A.M.C. wrote the manuscript, which was reviewed by all authors. Copy number and gene expression data is available from GEO (GSE35988).

[9]Compendia Bioscience, Ann Arbor, MI USA

Abstract

Characterization of the prostate cancer transcriptome and genome has identified chromosomal rearrangements and copy number gains/losses, including ETS gene fusions, *PTEN* loss and androgen receptor (*AR*) amplification, that drive prostate cancer development and progression to lethal, metastatic castrate resistant prostate cancer (CRPC)[1]. As less is known about the role of mutations[2–4], here we sequenced the exomes of 50 lethal, heavily-pretreated metastatic CRPCs obtained at rapid autopsy (including three different foci from the same patient) and 11 treatment naïve, high-grade localized prostate cancers. We identified low overall mutation rates even in heavily treated CRPC (2.00/Mb) and confirmed the monoclonal origin of lethal CRPC. Integrating exome copy number analysis identified disruptions of *CHD1*, which define a subtype of ETS fusionnegative prostate cancer. Similarly, we demonstrate that *ETS2*, which is deleted in ~1/3 of CRPCs (commonly through *TMPRSS2:ERG* fusions), is also deregulated through mutation. Further, we identified recurrent mutations in multiple chromatin/histone modifying genes, including *MLL2* (mutated in 8.6% of prostate cancers), and demonstrate interaction of the MLL complex with AR, which is required for AR-mediated signaling. We also identified novel recurrent mutations in the *AR* collaborating factor *FOXA1*, which is mutated in 5 of 147 (3.4%) prostate cancers (both untreated localized prostate cancer and CRPC), and showed that mutated *FOXA1* represses androgen signaling and increases tumour growth. Proteins that physically interact with AR, such as the *ERG* gene fusion product, FOXA1, MLL2, UTX, and ASXL1 were found to be mutated in CRPC. In summary, we describe the mutational landscape of a heavily treated metastatic cancer, identify novel mechanisms of AR signaling deregulated in prostate cancer, and prioritize candidates for future study.

Although localized prostate cancer is highly curable, more than 32,000 U.S. men die annually of metastatic disease. Androgen-deprivation therapy results in rapid responses in men with metastatic prostate cancer, however nearly all patients eventually progress (castrate resistant prostate cancer [CRPC]). Although CRPC was thought to be androgen signaling independent, recent evidence demonstrates that androgen signaling is often maintained through varied mechanisms (reviewed in[1,5]). Gene expression and copy number profiling studies have identified recurrent gene fusions, chromosomal gains and losses, and deregulated pathways in prostate cancer [1]. Resequencing studies have characterized the mutational spectrum of prostate cancer[3,4,6], and the genomes of seven localized prostate cancers have been reported by Berger *et al*. [7]. More recently, Kumar *et al*. reported the exomes of xenografts from 16 CRPC cases[2].

Here, we sequenced the exomes of 50 lethal heavily pretreated CRPCs (WA2-60) obtained at rapid autopsy[8], including three distinct sites in the same patient, and eleven treatment naïve, high-grade localized prostate cancers (T1-T97) (Supplementary Table 1). Sequencing results, including coverage statistics, mutation rates, validation rates, mutational spectrum, confirmation of the monoclonal origin of CRPC, and overlap with mutations observed in previous studies are provided in the Supplementary Results, Supplementary Figures 1–6 & Tables 2–6.

We used exome sequencing data to identify somatic copy number alterations [9] (see **Methods** and Supplementary Fig. 7 and Supplementary Tables 7–9), and as shown in Supplementary Fig. 8 we identified recurrent aberrations previously associated with prostate cancer development and progression (Supplementary Results). We additionally performed array CGH (aCGH) copy number and gene expression profiling on a matched cohort of benign prostate tissues, localized prostate cancers (3/59 sequenced) and 35 CRPCs (31/35 sequenced) (Supplementary Table 10). Profiles were uploaded into Oncomine (www.oncomine.com) for automated data processing, analysis and visualization, and are available for exploration. aCGH profiles were similar to copy number analysis by exome sequencing and to other prostate cancer profiling studies available in Oncomine (Supplementary Fig. 9). Global gene expression profiles were similar to previous studies (analyses available in Oncomine), with exceptions described in the Supplementary Results and Supplementary Fig. 10. Finally, we performed transcriptome sequencing of 11 prostate cancer cell lines to identify likely somatic variants (see Supplementary Results, Methods and Tables 11–15).

From our exome data, we identified nine genes that were significantly mutated (false discovery rate ≤ 0.10) (Fig. 1, Supplementary Tables 16&4), six of which have been reported as recurrently mutated in prostate cancer: *TP53*, *AR*, *ZFHX3*, *RB1*, *PTEN* and *APC*. Three significantly mutated genes do not have described roles in prostate cancer: *MLL2*, *OR5L1* and *CDK12*. *MLL2* encodes a H3K4-specific histone methyltransferase that is recurrently mutated in multiple cancers and *CDK12* was recently identified as significantly mutated in ovarian serous carcinoma[10]. Additionally, using several approaches, we identified multiple significantly mutated pathways, including WNT signaling, and a PTEN interaction network (Supplementary Figure 11 & Tables 17&18); observations on significantly mutated genes and pathways are provided in the Supplementary Results.

Multiple candidate driver mutations in genes associated with AR signaling, DNA damage response, histone/chromatin modification, the spindle checkpoint, and classical tumour suppressors and oncogenes were also identified (Fig. 1). For example, we identified two deleterious mutations in *PRKDC* (I1137fs and E640*), which encodes the catalytic subunit of the DNA-dependent protein kinase involved in DNA double strand break repair and recombination, in patient T96, who had an extremely aggressive localized prostate cancer. Additional mutated genes in these pathways are described in the Supplementary Results.

To identify potential CRPC drivers, we considered genes with recurrent high-level gains or losses present in peaks of global copy number change, and compared results to mutated genes (Supplementary Fig. 12), as described in the Supplementary Results. Thus, we were intrigued by the peak of copy number loss on chr 5q21 (Fig 2a and Supplementary Fig. 12) harboring *CHD1*, which encodes an ATP-dependent chromatin-remodeling enzyme reported as deregulated in 3 of 7 prostate cancer genomes by Berger *et al*. (one somatic splice-site mutation and two rearrangements)[7]. As described in the Supplementary Results & Figure 13, across our exome and aCGH copy number analysis, we identified focal deletion/mutation of *CHD1* (*CHD1*$^{-}$) in 10/119 (8%) prostate cancers, which was significantly associated with ETS gene fusion negative (ETS^{-})status (two sided Fisher's exact test,

p=0.02). Association of *CHD1* gene expression and genomic *CHD1*$^{-}$ status is shown in Supplementary Fig. 13b.

We next analyzed the association between *CHD1*$^{-}$ and ETS status in three prostate cancer aCGH and nine expression profiling studies (totaling 835 additional cancers) using Oncomine (Supplementary Results). As shown in Supplementary Figure 14 and Table 19 and Figure 2b, in total, across 13 DNA and RNA based studies, we identified 50 of 954 (5.2%) prostate cancers as *CHD1*$^{-}$, 48 of which (96%) were ETS^{-} ($p<0.0001$, two sided Fisher's exact test). Together, our integrated analysis identifies *CHD1*$^{-}$/ ETS^{-} as a novel prostate cancer subtype.

ETS genes have a central role in prostate cancer, most commonly through fusion to androgen driven genes (i.e. *TMPRSS2:ERG*), and as the majority of ETS gene fusion positive (ETS^{+}) CRPCs retained marked over-expression of the rearranged ETS gene (*ERG*, *ETV1* or *ETV5*), our results support active androgen signaling in the majority of these men (Supplementary Fig. 13b). We next further explored the role of ETS genes in prostate cancer by evaluating our dataset for aberrations in additional ETS genes. Importantly, two CRPCs harbored deleterious mutations in *ETV3*, (P327fs in WA56 and W38* in WA26, both ETS^{+}), which does not have a described role in prostate cancer. In addition, we were intrigued by the mutation of *ETS2* (R437C) in WA30 (ETS^{-}), as *ETS2* shows a similar DNA binding motif as *ERG*[11] and is located immediately telomeric to *ERG* (head-to-head orientation) in the commonly deleted region in *TMPRSS2:ERG* fusions through deletion. We also identified focal deletions extending telomeric from *ERG* in ERG^{+} cancers, as well as focal deletion of *ETS2* in WA31, which shows outlier under-expression of *ETS2* (Supplementary Results, & Fig 15). Additionally, the R437C mutation in *ETS2* occurs in the ETS domain at a DNA contacting residue conserved in class I ETS transcription factors[11], which include all ETS genes known to be involved in gene fusions in prostate cancer (Fig. 2c). Given observations that prostate cancers with *TMPRSS2:ERG* fusions through deletion may be more aggressive than those with fusions through insertion, we and others have speculated that the intervening region may harbor tumour suppressors, including *ETS2*[12–14]. As shown in Fig 2d, we demonstrate that over-expression of wild type *ETS2* results in decreased migration, invasion and proliferation in VCaP cells, while the R437C mutation has opposite effects, supporting a potential tumour suppressive role for *ETS2*.

In addition to *MLL2* and *CHD1*, our integrated analysis identified mutations and copy number aberrations in multiple other genes involved in chromatin/histone modification (Fig. 1), including multiple members of the MLL complex (see Supplementary Results and Fig 3). Besides *CHD1*, which shows deregulation in both localized prostate cancer and CRPC (Fig. 2 and Supplementary Figs. 13&14), mutations of other chromatin/histone remodeling genes were infrequent in localized prostate cancer and concentrated in a single sample (T97, Fig. 1). Hence, we hypothesized that the mutated chromatin/histone remodelers we identified may mediate AR signaling through interaction. Thus, we immunoprecipitated endogenous AR from VCaP cells (ERG^{+} CRPC, active AR signaling) and blotted for members of the MLL complex (MLL2, MLL, ASH2L), UTX, ASXL1 and CHD1. FOXA1, a known direct interacting AR cofactor[15], and EZH2 (a H3K27 histone methyltransferase over-expressed in CRPC), were evaluated as positive and negative controls, respectively. As shown in Figure

3a, members of the MLL complex, UTX and ASXL1 all interact with AR, while interaction with CHD1 was not observed. Reverse immunoprecipitation confirmed interactions between AR and MLL, MLL2, ASH2L and FOXA1 (Supplementary Fig. S16a).

As the MLL complex is implicated in epigenetic transcriptional activation, we studied its role in AR signaling. RNA interference of *MLL* or *ASH2L* using independent siRNAs (Supplementary Fig. 16b) significantly inhibited AR signaling, as assessed by inhibition of R1881 (synthetic androgen) stimulation of *KLK3* (*PSA*) expression, with two siRNAs each against *MLL* or *ASH2L* inhibiting *KLK3* expression at 24 hours by > 7.5 fold (each $p<0.001$) (Fig. 3b). Together, our data suggest that aberrations in AR and interacting proteins, including chromatin/histone remodelers, ETS genes (exemplified by ERG, which directly interacts with AR[16]) and known AR co-regulators including *FOXA1* (see below), are common in CRPC (Fig. 3c).

Given the central role of AR signaling in CRPC and the selection for aberrations in AR occurring in CRPC, we were intrigued by the identification of a somatic 2 bp insertion in *FOXA1* (S453fs) in the localized prostate cancer sample T12, and 340fs and P358fs indels in DU-145 and LAPC-4 (identified by transcriptome sequencing), respectively, given the well described role of *FOXA1* in AR signaling[17–22]. Thus, we screened 101 localized and 46 CRPCs (including foci from all exome sequenced CRPCs), and identified somatic mutations of *FOXA1* in 4 localized prostate cancers and 1 CRPC (total 5 of 147, 3.4%). Importantly, 4 of the 5 mutations, as well as both indels identified in the transcriptome screen, occurred in the C-terminal transactivating domain (Fig. 4a). As described in the Supplementary Results, we demonstrate that stable expression in LNCaP cells of either wild type *FOXA1* or observed *FOXA1* mutants increase proliferation in the presence of androgen (Fig 4b&c), represses the AR transcriptional program (Fig. 4d), and result in increased soft agar colony (Supplementary Fig 17) and xenograft growth (Fig 4e).

Our integrated, exome-based profiling of the mutational landscape of CRPC is notable for representing a large cohort of heavily pre-treated patients with lethal metastatic disease, which are not commonly studied, and provides insights into the resistance mechanisms that evolve in refractory tumours. Additionally, we identified a diverse series of potentially driving mutations and copy number alterations in both known and novel genes and pathways, including *FOXA1*. Lastly, our integrative genomics dataset provides a useful resource for the study of lethal prostate cancer, as well as determinants of, or resistance mechanisms to, radiation and chemotherapy.

Methods Summary

See Supplementary Methods for source of prostate tissues and cell lines, nucleic acid isolation, exome and transcriptome sequencing and data analysis, mutation validation by Sanger sequencing, aCGH and DNA microarray expression profiling, *ETS2* in vitro experiments, AR interactor immunoprecipitation, western blotting, and siRNA experiments, *FOXA1* screening and in vitro and in vivo experiments.

Supplementary Material

Refer to Web version on PubMed Central for supplementary material.

Acknowledgments

The authors thank the patients and families who participated in the Rapid Autopsy Program. The authors thank Chandan Kumar, Jay Shendure, Mark Chaisson, and Ali Mortazavi for assistance with next generation sequencing data analysis, Karen Giles for assistance with manuscript preparation, and Sooryana Varambally, Anastasia Yocum, Terrence Barrette and Matthew Iyer for technical assistance. Supported in part by the NIH S.P.O.R.E. (P50 CA69568) to K.J.P. and A.M.C., the Early Detection Research Network (U01 CA111275 and U01 CA113913) to A.M.C., R01CA132874 and the National Functional Genomics Center (W81XWH-09-2-0014) to A.M.C. A.M.C. and K.J.P. are supported by the Prostate Cancer Foundation and are American Cancer Society Clinical Research Professors and A. Alfred Taubman Scholars. A.M.C. is supported by the Doris Duke Foundation. D. R. is supported by a DOD Postdoctoral Award (W81XWH-11-1-0339). J.R.P. is supported by a DOD Predoctoral Award (PC094290). S.A.T. and J.C.B. were supported by Young Investigator Awards from the Prostate Cancer Foundation.

References

1. Shen MM, Abate-Shen C. Molecular genetics of prostate cancer: new prospects for old challenges. Genes Dev. 2010; 24:1967–2000. [PubMed: 20844012]
2. Kumar A, et al. Exome sequencing identifies a spectrum of mutation frequencies in advanced and lethal prostate cancers. Proc Natl Acad Sci U S A. 2011; 108:17087–17092. [PubMed: 21949389]
3. Robbins CM, et al. Copy number and targeted mutational analysis reveals novel somatic events in metastatic prostate tumours. Genome Res. 2010
4. Taylor BS, et al. Integrative genomic profiling of human prostate cancer. Cancer Cell. 2010; 18:11–22. [PubMed: 20579941]
5. Attard G, Reid AH, Olmos D, de Bono JS. Antitumouractivity with CYP17 blockade indicates that castration-resistant prostate cancer frequently remains hormone driven. Cancer Res. 2009; 69:4937–4940. [PubMed: 19509232]
6. Kan Z, et al. Diverse somatic mutation patterns and pathway alterations in human cancers. Nature. 2010; 466:869–873. [PubMed: 20668451]
7. Berger MF, et al. The genomic complexity of primary human prostate cancer. Nature. 2011; 470:214–220. [PubMed: 21307934]
8. Rubin MA, et al. Rapid (“warm”) autopsy study for procurement of metastatic prostate cancer. Clin Cancer Res. 2000; 6:1038–1045. [PubMed: 10741732]
9. Lonigro RJ, et al. Detection of somatic copy number alterations in cancer using targeted exome capture sequencing. Neoplasia. 2011; 13:1019–1025. [PubMed: 22131877]
10. Integrated genomic analyses of ovarian carcinoma. Nature. 2011; 474:609–615. [PubMed: 21720365]
11. Wei GH, et al. Genome-wide analysis of ETS-family DNA-binding in vitro and in vivo. Embo J. 2010; 29:2147–2160. [PubMed: 20517297]
12. Demichelis F, et al. Distinct genomic aberrations associated with ERG rearranged prostate cancer. Genes Chromosomes Cancer. 2009; 48:366–380. [PubMed: 19156837]
13. Perner S, et al. TMPRSS2:ERG fusion-associated deletions provide insight into the heterogeneity of prostate cancer. Cancer Res. 2006; 66:8337–8341. [PubMed: 16951139]
14. Yoshimoto M, et al. Three-color FISH analysis of TMPRSS2/ERG fusions in prostate cancer indicates that genomic microdeletion of chromosome 21 is associated with rearrangement. Neoplasia. 2006; 8:465–469. [PubMed: 16820092]
15. Yu X, et al. Foxa1 and Foxa2 interact with the androgen receptor to regulate prostate and epididymal genes differentially. Ann N Y Acad Sci. 2005; 1061:77–93. [PubMed: 16467259]
16. Yu J, et al. An integrated network of androgen receptor, polycomb, and TMPRSS2-ERG gene fusions in prostate cancer progression. Cancer Cell. 2010; 17:443–454. [PubMed: 20478527]

17. Gao N, et al. The role of hepatocyte nuclear factor-3 alpha (Forkhead Box A1) and androgen receptor in transcriptional regulation of prostatic genes. Mol Endocrinol. 2003; 17:1484–1507. [PubMed: 12750453]
18. Wang Q, et al. A hierarchical network of transcription factors governs androgen receptor-dependent prostate cancer growth. Mol Cell. 2007; 27:380–392. [PubMed: 17679089]
19. Wang Q, et al. Androgen receptor regulates a distinct transcription program in androgen-independent prostate cancer. Cell. 2009; 138:245–256. [PubMed: 19632176]
20. Lupien M, et al. FoxA1 translates epigenetic signatures into enhancer-driven lineage-specific transcription. Cell. 2008; 132:958–970. [PubMed: 18358809]
21. Sahu B, et al. Dual role of FoxA1 in androgen receptor binding to chromatin, androgen signalling and prostate cancer. Embo J. 2011; 30:3962–3976. [PubMed: 21915096]
22. Zhang C, et al. Definition of a FoxA1 Cistrome that is crucial for G1 to S-phase cell-cycle transit in castration-resistant prostate cancer. Cancer Res. 2011; 71:6738–6748. [PubMed: 21900400]
23. Werner MH, et al. Correction of the NMR structure of the ETS1/DNA complex. J Biomol NMR. 1997; 10:317–328. [PubMed: 9460239]

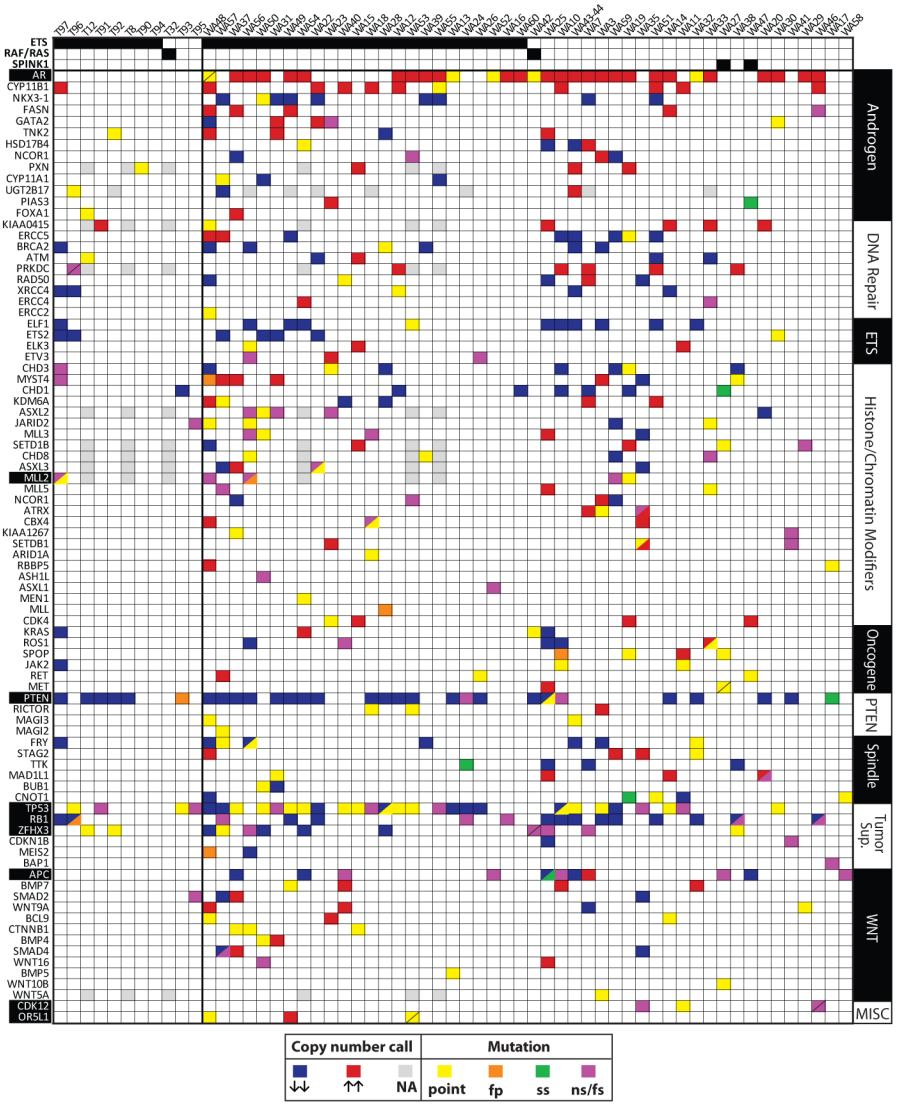

Figure 1. Integrated mutational landscape of lethal metastatic castrate resistant prostate cancer (CRPC)

Exomes of 50 CRPC (WA3-WA60; three foci from WA43) and 11 high-grade untreated localized prostate cancers (T8-T97) were sequenced to identify somatic mutations and copy number alterations. Heatmap of high-level copy number alterations and non-synonymous mutations. Samples are stratified by ETS status in localized prostate cancer and CRPCs, and ordered by the total number of aberrations in shown genes. ETS gene fusions, RAF/RAS family aberrations, and *SPINK1* outlier expression is indicated for all samples (black is present). For each gene, aberrations as indicated are shown (two aberrations in the same gene are indicated by divided boxes). Significantly mutated genes have white names. Mutations in the hypermutated sample WA16 are not shown.

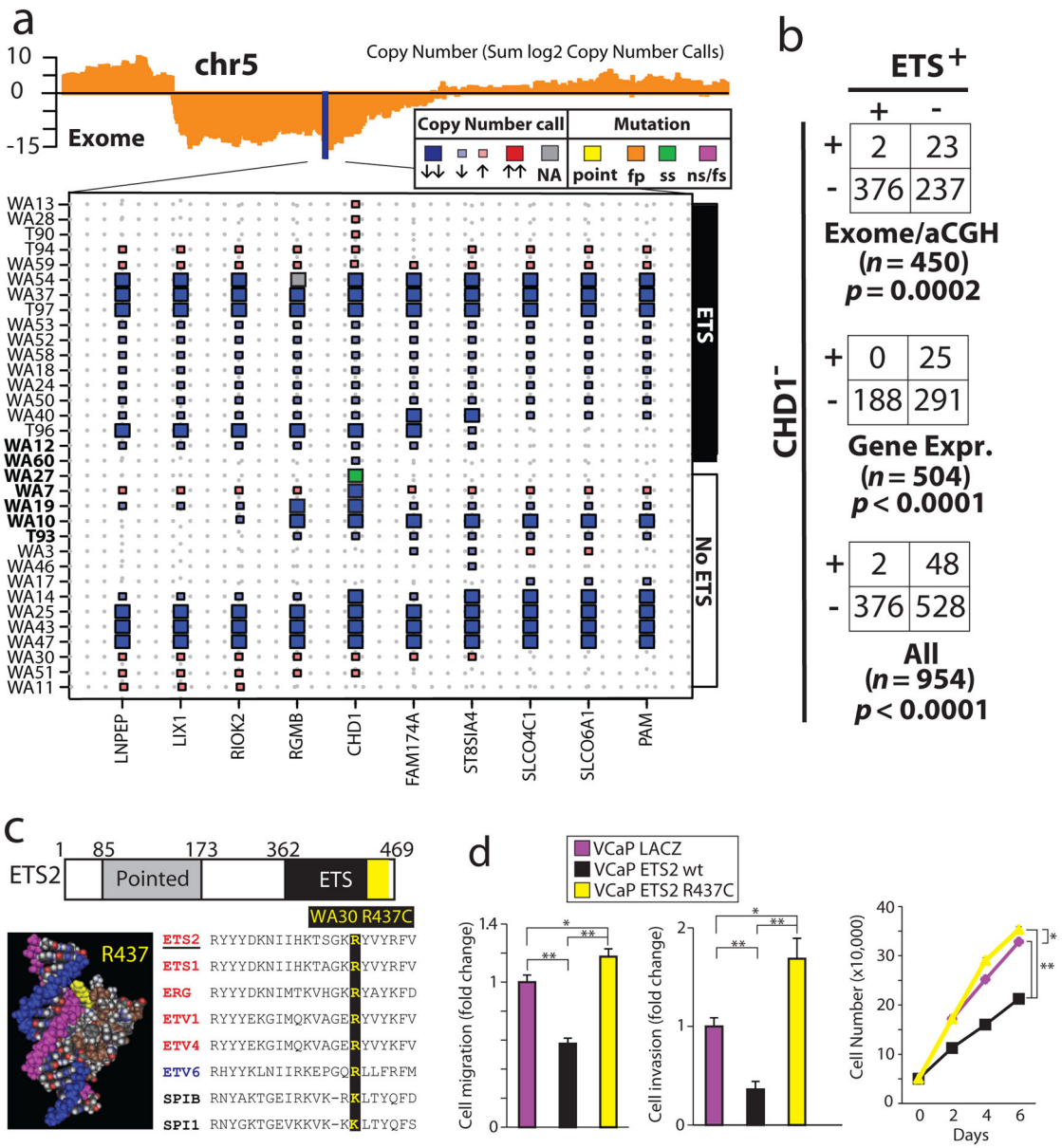

Figure 2. Integrated exome sequencing and copy number analysis highlights novel aspects of ETS genes in prostate cancer biology: deregulation of *CHD1* and *ETS2*

a–b. *CHD1* deregulation through deletion or mutation in ETS fusion negative (ETS^{-}) prostate cancer. **a**. Genome wide copy number analysis identified a peak of copy number loss on chr5q21 centered on *CHD1* (upper panel, blue bar). The expanded view shows individual samples as rows, with indicated genes represented by boxes. The area and size of each box indicates the copy number call (see legend). Only samples with at least one gene in the region with a called copy number gain/loss are shown, and missing boxes indicate that gene has no called copy number gain/loss. Mutations in *CHD1* are indicated according to the legend and samples with focal deletions or mutation of *CHD1* are bolded. **b**. Co-occurrence of *CHD1* deregulation (*CHD1*$^{-}$) and ETS^{+} from the current exome study and 3 aCGH

studies (Exome/aCGH), 9 gene expression profiling studies (Gene Expr.), and all studies (All). The total number of samples in each set (*n*) is shown, and two sided Fisher's exact tests were performed. **c–d.** *ETS2* is a prostate cancer tumour suppressor deregulated through deletion and mutation. **c**. WA30 (yellow) harbored a R437C mutation that disrupts a residue conserved in class I ETS transcription factors (red), but not in class IIb or III factors (blue and black, respectively). R437 (yellow) contacts DNA (blue and magenta) in the ETS domain (brown), as shown by the structure of the homologous residue in ETS1 (R409, PDB: 3MFK[23]). **d**. VCaP prostate cancer cells (*ERG*$^{+}$) stably expressing *ETS2* (wild type [wt] or R437C) or *LACZ* were evaluated for migration (left panel, *n*=8), invasion (middle panel, *n*=12) and proliferation (right panel, *n*=4). For migration and invasion, fold change relative to VCaP *LACZ* was plotted. For each experiment, mean ± S.E. is plotted; * and ** indicate $p<0.05$ or <0.001 from two tailed t-tests.

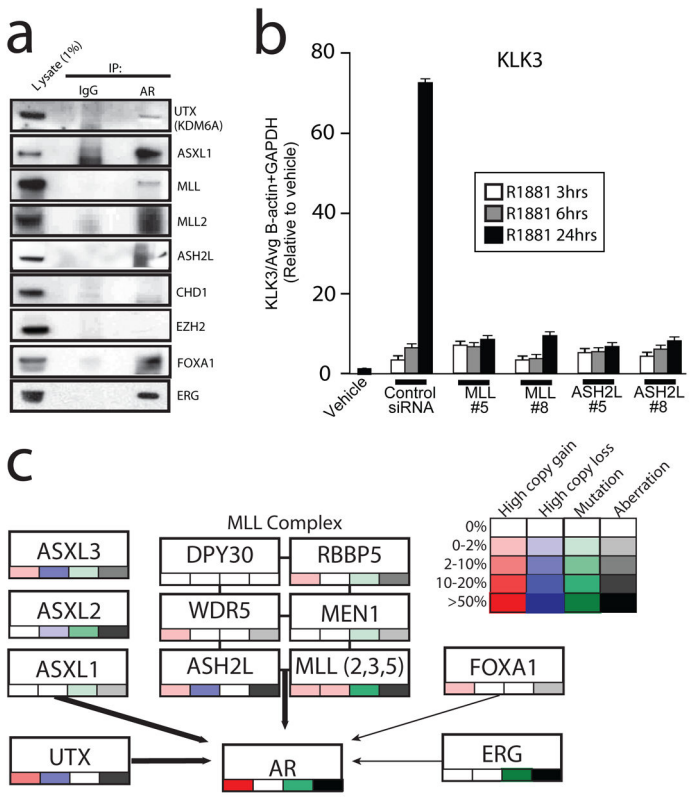

Figure 3. Castrate resistant prostate cancer (CRPC) harbors mutational aberrations in chromatin/histone modifiers that physically interact with AR

Deregulation through mutation or high-level copy aberrations of multiple chromatin/histone modifying genes was identified (see Fig. 1). **a**. Interaction of deregulated chromatin/histone modifiers with AR. AR (or IgG as control) was immunoprecipitated from VCaP cells and Western blotting for the indicated chromatin/histone modifier was performed. 1% lysate was used as control. EZH2 and FOXA1 were used as negative and positive controls, respectively. **b**. VCaP cells were treated with siRNAs against *MLL* or *ASH2L* (or non-targeting as control), starved, stimulated with vehicle or 1nm R1881 for the indicated times and harvested. qPCR for *KLK3* (PSA) expression (relative to vehicle) is plotted (*n*=3, mean + S.E.). **c.** Summary of genes interacting with AR that are deregulated in CRPC. Frequency of high copy alterations, somatic mutations, and both aberration types according to the color scales, are shown for chromatin/histone modifiers, the AR collaborating factor *FOXA1* and *ERG*. MLL aberration frequency includes *MLL*, *MLL2*, *MLL3* and *MLL5*. Genes encoding AR interactors identified in this and previous studies are indicated by bold and regular arrows, respectively.

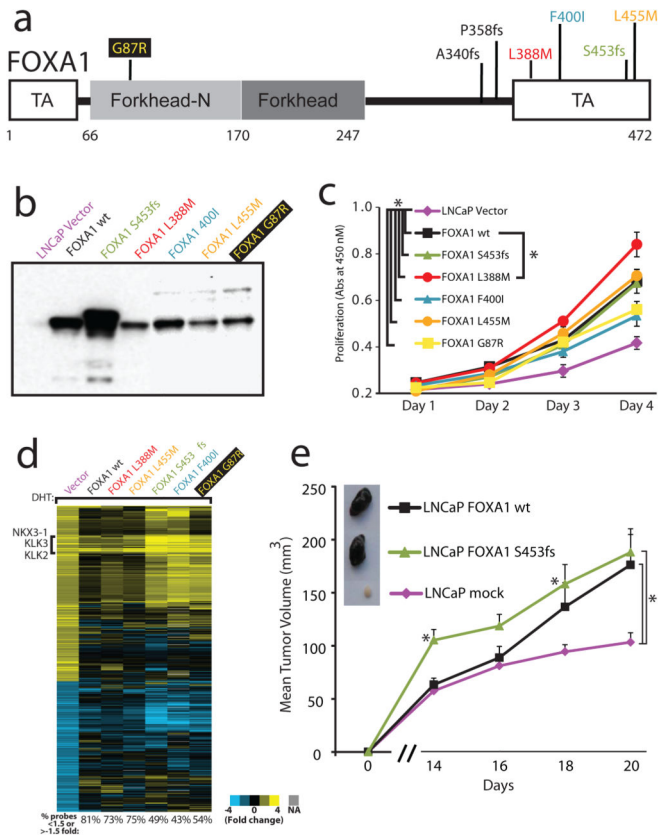

Figure 4. Recurrent mutations in the androgen receptor (AR) collaborating factor *FOXA1* promote tumour growth and affect AR signaling

a. Exome sequencing and subsequent screening of 147 prostate cancers (101 treatment naïve localized and 46 CRPCs) identified 5 samples with *FOXA1* mutations, and transcriptome sequencing of 11 prostate cancer cell lines identified indels in LAPC-4 and DU-145 (shown in black). Locations of mutations are indicated on the domain structure of FOXA1 (TA= transactivation domains). **b.** Wild type *FOXA1* (wt, black) and *FOXA1* mutants observed in clinical samples were stably expressed in LNCaP cells as N-terminal FLAG fusions (empty vector, purple, as control). Western blotting with anti-FLAG antibody confirmed expression. **c.** Cell proliferation in 1% charcoal-dextran stripped serum with 10 nM DHT was measured by WST-1 colorimetric assay. Mean + S.E. (*n*=4) is plotted. **d**. *FOXA1* wild-type and mutations identified in prostate cancer repress androgen signaling. Indicated LNCaP cells were treated with vehicle or 10 nM DHT for 48 hrs prior to expression profiling. The heatmap shows probes with >2 fold change after DHT stimulation in LNCaP vector DHT/vehicle cells. Probes were clustered using centroid linkage. For each *FOXA1* mutant (or wild-type) DHT/vehicle condition, the percentage of filtered probes showing <1.5 or >-1.5 fold change (indicating repression) is indicated. **e**. Subcutaneous xenografts were generated from LNCaP cells stably expressing *LACZ* (control, purple), or N-terminally HA-tagged *FOXA1* (wild type [wt] or S453fs). Tumour volume is plotted and representative tumours are shown. Mean + S.E. (*n*=3) is plotted; * indicates $p < 0.05$ from two tailed t-test.